Inorganic Chemistry

Article

pubs.acs.org/IC

Synthesis and Electronic Structure of $Ru_2(Xap)_4$(Y-*gem*-DEE) Type Compounds: Effect of *Cross*-Conjugation

William P. Forrest,[†] Mohommad M. R. Choudhuri,[‡] Stefan M. Kilyanek,[§] Sean N. Natoli,[†] Boone M. Prentice,[†] Phillip E. Fanwick,[†] Robert J. Crutchley,[‡] and Tong Ren*[,†]

[†]Department of Chemistry, Purdue University, West Lafayette, Indiana 47907, United States

[‡]Department of Chemistry, Carleton University, Ottawa, Ontario K1S 5B6, Canada

[§]Department of Chemistry and Biochemistry, University of Arkansas, Fayettesville, Arkansas 72701, United States

Supporting Information

ABSTRACT: Reported in this Article are the preparation and characterization of a series of new Ru_2(II,III) compounds bearing one *cross*-conjugated σ-*geminal*-diethynylethene ligand (*gem*-DEE), namely, $Ru_2(Xap)_4$(Y-*gem*-DEE) (*Xap* = *N*,*N*′-anilinopyridinate (*ap*) or 2-(3,5-dimethoxy)anilinopyridinate (DiMeO*ap*), and Y = Si^iPr_3 (**1**) or H (**2**)) and $[Ru_2(ap)_4]_2(\mu$-*gem*-DEE) (**3**). Compounds **1**−**3** were characterized by spectroscopic and voltammetric techniques as well as the single crystal X-ray diffraction study of **2a**. The X-ray structural data of **2a** and the spectroscopic/voltammetric data of compounds **1** and **2** indicate that the *gem*-DEE ligands are similar to simple alkynyls in their effects on the molecular and electronic structures of the $Ru_2(Xap)_4$ moiety. Similar to the previously studied $[Ru_2(ap)_4]_2(\mu$-$C_{2n})$ type compounds, dimer **3** exhibits pairwise $1e^-$ oxidations and reductions, albeit the potential splits within the pair ($\Delta E_{1/2}$) are significantly smaller than those of $[Ru_2(ap)_4]_2(\mu$-$C_4)$. The electronic absorption spectra of the reduced and oxidized derivatives of **1a** and **3** were determined using spectroelectrochemistry methods. No discernible intervalence charge transfer transition (IVCT) was detected in the near-IR spectrum for either $\mathbf{3}^-$ or $\mathbf{3}^+$, suggesting that the Ru_2−Ru_2 coupling in these mixed-valence states is weak. DFT calculations on a model compound of **3** yielded six singly occupied molecular orbitals (SOMOs), which have Ru_2 contributions similar to those previously calculated for the $[Ru_2(ap)_4]_2(\mu$-$C_{2n})$ type compounds. Among six SOMOs, SOMO-2 is the only one containing substantial $d\pi$−π(*gem*-DEE) character across the entire Ru_2-μ-*gem*-DEE-Ru_2 linkage, which explains the weakened Ru_2−Ru_2 coupling.

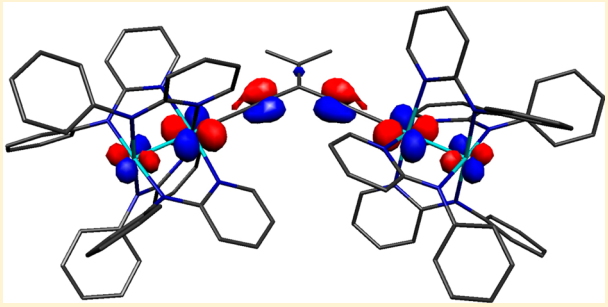

INTRODUCTION

Organometallic compounds with conjugated carbon-rich backbones have been studied as prospective molecular wires[1,2] and nonlinear optical (NLO) chromophores.[3] Much of the research during the past 20 years on molecular wires has been based on *linearly* conjugated σ-oligoen-diyl -(C═C)$_n$- or σ-oligoyn-diyl -(C≡C)$_n$- ligands capable of facilitating facile charge transfer.[2,4] Notable examples of the [M]-(C≡C)$_n$-[M] type compounds include M as Re,[5] Fe,[6] Ru,[7] Pt,[8] and Ru_2,[9−13] where significant electronic couplings between the two [M] termini mediated by the polyyn-diyl bridges were demonstrated in bulk media based on voltammetric and spectroscopic studies. Though less studied compared to oligoyn-diyl bridged compounds, bimetallic compounds bridged with oligoen-diyl have been prepared with M = Ru[14] and Fe,[15] where significant M—M couplings were uncovered as well.

In contrast to the aforementioned successes based on transition metal σ-oligoyn-diyls, far less investigated are complexes containing nonlinear or branched carbon-rich linkers, such as the *cross*-conjugated[16,17] and cruciform types.[18] The concept of cross-conjugation has been around for quite some time and was defined as "a compound possessing three unsaturated groups, two of which although conjugated to a third unsaturated center are not conjugated to each other" according to Phelan and Orchin.[19] Recent synthetic advances, primarily from the laboratories of Diederich[16,20] and Tykwinski,[17,21] have made it possible to explore cross-conjugated nonlinear eneyne and enediyne scaffolds, which have drawn considerable interest recently due to their novel optoelectronic properties.[17,22] Transition metal complexes with eneyne or enediynes as σ-alkynyl ligands are very rare,[12] and ones based on σ-*geminal*-diethynylethene ligand (*gem*-DEE) were first studied in macrocyclic Pt(II) compounds by the laboratory of Tykwinski.[23] More recently, diruthenium compounds bridged by cross-conjugated penta-1,4-diyn-3-one and its derivatives were reported by Bruce and co-workers.[24]

As the first examples of *gem*-DEE compounds with a redox-active metal center, our laboratory recently reported a series of *trans*-$Ru_2(DMBA)_4$(*gem*-DEE)$_2$, where DMBA is *N*,*N*′-dime-

Received: June 11, 2015
Published: July 23, 2015

DOI: 10.1021/acs.inorgchem.5b01315
Inorg. Chem. 2015, 54, 7645−7652

thylbenzamidinate.[25] Subsequently, *trans*-[M(cyclam)(*gem*-DEE)$_2$]OTf type compounds with M as Cr(III)[26] and Fe(III)[27] were prepared and investigated. In all three cases, weak electronic couplings between ferrocenyl substituents of *gem*-DEE across the metal center were inferred from voltammetric data. In order to access the bridged *gem*-DEE species, our attention has turned to the Ru$_2$(*ap*)$_4$(II,III) type building blocks, with which we have had great success in achieving linear oligoyn-diyl bridged Ru$_2$(*ap*)$_4$-C$_{2n}$-Ru$_2$(*ap*)$_4$ compounds (n = 1−10).[9,11,13] First alkynyl compounds containing a Ru$_2$(*ap*)$_4$ unit, Ru$_2$(*ap*)$_4$(C$_2$Y)$_x$ (x = 1 and 2), were described by Chakravarty and Cotton,[28] and the relevant synthetic chemistry has been explored extensively by both the laboratories of Kadish and Bear[29,30] and Ren.[31−33] Described herein are the preparation of two different types of Ru$_2$-*gem*-DEE compounds (Chart 1): (i) Ru$_2$-mono-*gem*-DEE compounds (**1** and **2**),

Chart 1. New Ru$_2$(*ap*)$_4$-*gem*-DEE Compounds

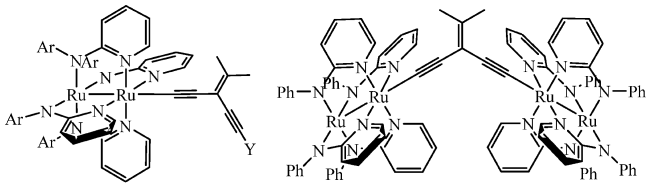

Y= -Si^{i}Pr$_3$, **1a** (*ap*), **1b** (DiMeO*ap*)
Y= H; **2a** (*ap*), **2b** (DiMeO*ap*)

3

Ru$_2$(X*ap*)$_4$(Y-*gem*-DEE) (X*ap*: *ap* = *N*,*N*′-anilinopyridinate (**a**) and DiMeO*ap* = 2-(3,5-dimethoxyanilino)pyridinate (**b**); Y = -Si^{i}Pr$_3$ (**1**) and −H (**2**) and *gem*-DEE = *geminal*-diethynylethene); and (ii) dimeric [Ru$_2$(*ap*)$_4$]$_2$(*μ*-*gem*-DEE) (**3**). The latter compound allows for a direct assessment of the electronic coupling between the two Ru$_2$(II,III) centers through the cross-conjugated *gem*-DEE bridge based on voltammetry and spectroelectrochemistry.

RESULTS AND DISCUSSION

Synthesis of Ru$_2$(Xap)$_4$(Y-*gem*-DEE) Compounds. Analogous to the preparative methods for Ru$_2$(*ap*)$_4$(C$_2$Ph)[28] and the oligoynyl-silyl derivatives Ru$_2$(*ap*)$_4$(C$_{2m}$SiR$_3$),[31,34] the reaction between 1 equiv of Ru$_2$(*ap*)$_4$Cl and 1.5 equiv of Li-*gem*-DEE-Si^{i}Pr$_3$ yielded compound **1a** (Scheme 1) as a

Scheme 1. Preparation of Compounds 1a/b and 2a/b

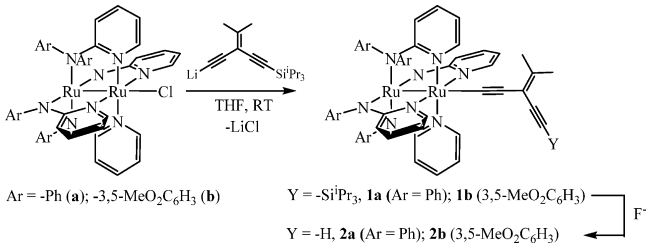

brownish-green solid in excellent yield (93%). Because of low to fair solubility of **1a** in common organic solvents, Ru$_2$(DiMeO*ap*)$_4$(^{i}Pr$_3$Si-*gem*-DEE) (**1b**) was similarly prepared from the reaction between 1 equiv of Ru$_2$(DiMeO*ap*)$_4$Cl and 1.5 equiv of Li-*gem*-DEE-Si^{i}Pr$_3$ in a yield of 77%. Both compounds **1a** and **1b** can be readily desilylated using aqueous (n-Bu)$_4$NF (TBAF) in THF overnight to yield compounds **2a** and **2b**, respectively. Alternatively, compounds **2a** and **2b** can also be obtained from the reactions between Ru$_2$(X*ap*)$_4$Cl and Li-*gem*-DEE-H. However, several byproducts also appeared in such reactions, which necessitated tedious column separation.

All Ru$_2$(X*ap*)$_4$ mono-*gem*-DEE compounds (**1** and **2**) have room-temperature effective magnetic moments (μ_{eff}) ranging between 3.67 and 3.80 μ_B, suggesting a S = 3/2 ground state that typifies Ru$_2$(*ap*)$_4$(C≡CR) type compounds.[31,34] Based on the studies of other Ru$_2$(II,III) systems, the ground state configuration for both compounds **1** and **2** is $\sigma^2\pi^4\delta^2(\pi^*\delta^*)^3$ and the Ru−Ru bond order is 2.5.[28,31,34,35] Due to their paramagnetic nature, compounds **1** and **2** cannot be unambiguously characterized using ^{1}H NMR technique. Instead, they were characterized via electrochemical (CV and DPV) and spectroscopic (vis−near-IR and FT-IR) analyses, high-resolution nanoelectrospray mass spectrometry (HR-nESI-MS), elemental analyses, and the single crystal X-ray diffraction study of **2a**.

Synthesis of [Ru$_2$(ap)$_4$]$_2$(*μ*-*gem*-DEE) (3). Similar to the preparative method for the [Ru$_2$(*ap*)$_4$]$_2$(*μ*-C$_{2n}$) type compounds with short oligoyn-diyl bridge ($n \leq 3$),[9,11] the initial attempt at preparation of **3** was the reaction between 2 equiv of Ru$_2$(*ap*)$_4$Cl and 1.2 equiv of Li-*gem*-DEE-Li. Indicative of dimer formation, the reaction mixture turned from green to purple. However, the isolated product was the butadiyn-diyl bridged dimer [Ru$_2$(*ap*)$_4$]$_2$(*μ*-C$_4$) (authenticated via nESI-MS, m/z 1809, corresponding to [M + H]$^+$) instead of the desired compound **3**. It became clear from the failed attempt that the bridging *gem*-DEE ligand was undergoing scission/rearrangement chemistry *in situ*, as a result of the two methyl substituents in the 1,1′-positions of the *gem*-DEE ligand being susceptible to excess basicity because of the use of *n*BuLi.[36] However, several attempts using weaker bases including LiN^{i}Pr$_2$ (LDA), Na[N(SiMe$_3$)$_2$] and KC$_7$H$_7$ in place of *n*-BuLi were unsuccessful in producing the desired compound **3**. Subsequently, a reaction between 2 equiv of Ru$_2$(*ap*)$_4$Cl and 1 equiv of Li-*gem*-DEE-Li (generated from 1 equiv of H-*gem*-DEE-H and only 2.2 equiv of *n*-BuLi) resulted in the desired compound **3** as a purple-brown solid, albeit in a 7% yield after column purification. The low yield was attributed to the sensitivity of **3** toward both water and air, a surprise since the [Ru$_2$(*ap*)$_4$]$_2$(*μ*-C$_{2n}$) type compounds are very stable under ambient conditions.

Two successful methods were eventually identified for producing **3** in moderate to good yields. As shown in Scheme 2, the first preparative method is analogous to the

Scheme 2. Syntheses of Compound 3

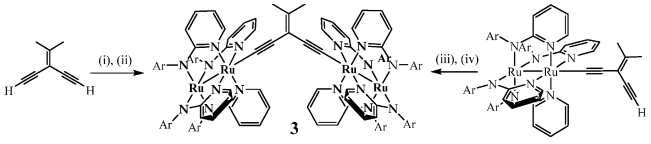

aforementioned successful attempt, where 1 equiv of Li-*gem*-DEE-Li (generated *in situ* from 1 equiv of H-*gem*-DEE-H and 2.2 equiv of *n*-BuLi at −78 °C) reacted with 2 equiv of Ru$_2$(*ap*)$_4$Cl at −78 °C. Upon crystallization from the reaction solution with the addition of distilled hexanes, the crude product was filtered under nitrogen atmosphere and washed with distilled Et$_2$O to provide compound **3** in 32% yield. Also shown in Scheme 2 is the second preparative method, which begins with treating 1 equiv of **1b** with 1.1 equiv of *n*-BuLi at

DOI: 10.1021/acs.inorgchem.5b01315
Inorg. Chem. 2015, 54, 7645−7652

−78 °C to yield Li-**1b**, to which was added 0.98 equiv of $Ru_2(ap)_4Cl$ at −78 °C. The reaction was stirred for 1 h at −78 °C and then was warmed to room temperature with continuous stirring overnight. The crude product precipitated from the reaction mixture and was collected via filtration. After thorough hexanes/Et_2O rinses, the solid collected was recrystallized from toluene/hexanes at −30 °C under nitrogen to yield compound **3** in 50% yield as a purple-brown, powder solid.

Dimeric compound **3** is quite unstable under ambient conditions and must be stored under N_2 atmosphere at room temperature or below. It has moderate solubility in MeCN, acetone and THF, and is very soluble in CH_2Cl_2 (degradation occurs after prolonged exposure) and toluene. The effective magnetic moment of **3** per $Ru_2(ap)_4$ is 4.52 μ_B, which is higher than the values reported for other $[Ru_2(Xap)_4]_2(\mu\text{-}C_{2n})$ species.[11] Although the paramagnetism prevents characterization through ^{1}H NMR spectroscopy, compound **3** was sufficiently characterized via electrochemical (CV and DPV) and spectroscopic (vis−near-IR and FT-IR) analyses, high-resolution nanoelectrospray mass spectrometry (HR-nESI-MS) and elemental analysis.

Crystal Structure of 2a. Direct confirmation of the formation of $Ru_2(ap)_4$-*gem*-DEE type compounds came from the single crystal X-ray diffraction study of **2a**. The molecular structure of **2a** is shown in Figure 1, along with the selected

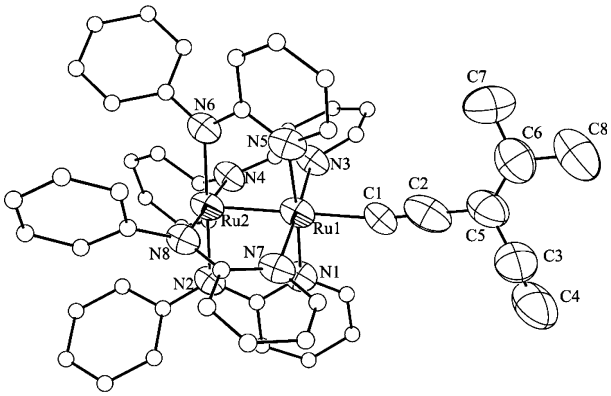

Figure 1. Structural plot of compound **2a** at 30% probability level. Hydrogen atoms were omitted for clarity. Selected bond lengths (Å) and angles (deg): Ru2−Ru1, 2.308(1); Ru1−N_{av}, 2.102[9]; Ru2−N_{av}, 2.050[9]; Ru1−C1, 2.07(1); C1−C2, 1.17(2); C3−C4, 1.13(3); C5−C6, 1.32(2); Ru2−Ru1−C1, 179.3(3); Ru1−C1−C2, 169(1); C1−C2−C5, 178(1); C2−C5−C3, 111(1).

bond lengths and angles. It is evident in Figure 1 that the *ap* ligands adopt the so-called (4,0)-arrangement around the Ru_2 core with all of the pyridine *N*-centers coordinating to the Ru(III) (Ru1), and all of the anilino N-centers coordinating to the Ru(II) (Ru2), which is consistent with previously studied $Ru_2(ap)_4(C{\equiv}CR)$ type compounds.[28,31,32,34] It should be noted that the assignment of Ru *formal* oxidation states is based on the nature of the ligand environment, while a +2.5 oxidation state is likely applicable to both Ru centers due to the strong Ru−Ru bonding.[37] It is also apparent from Figure 1 that the H-*gem*-DEE ligand is approximately coplanar with the framework defined by the N1−N2−N5−N6 linkage in **2a**.

The geometric parameters around the first coordination sphere of the Ru_2 core are comparable to those of other $Ru_2(ap)_4(C{\equiv}CR)$ type compounds.[28,31−34] The Ru1−Ru2 (2.308(1) Å) bond length in **2a** is within experimental error of that of $Ru_2(ap)_4(C{\equiv}CPh)$ (2.319(3) Å)[28] and other $Ru_2(ap)_4$ monoalkynyl compounds (2.316−2.330 Å),[31,32] which is consistent with a Ru−Ru bond order of 2.5. There is a significant difference between the two independent Ru−N bond lengths (N_p indicates the pyridine N atoms, while N_a indicates the anilino N atoms): (i) the averaged Ru1−N_p bond length is 2.102[9] Å, while (ii) the averaged Ru2−N_a bond length is 2.05[9] Å. The difference in the bond lengths can be attributed to the fact that the pyridine nitrogen is not as good of a donor as the anilino nitrogen.[31,34] The Ru1−C1 (2.07(1) Å) bond length in **2a** is identical to those previously reported for $Ru_2(ap)_4(C{\equiv}CR)$ (2.075−2.080 Å) type compounds within experimental errors. All of the aforementioned data indicate that the *gem*-DEE ligand behaves similarly to a simple alkynyl ligand in bonding to the $Ru_2(ap)_4$ core.

Electrochemical Studies. The redox characteristics of compounds **1**−**3** were carefully examined with both cyclic (CV) and differential pulse volatammetry (DPV). The CV and DPV plots of compounds **1a**, **2b**, and **3** are provided in Figure 2, while the potential data for compounds **1**−**3** are collected in

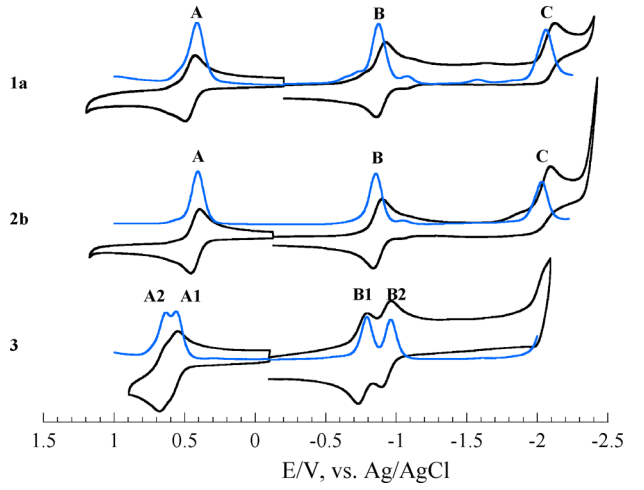

Figure 2. CVs (black) and DPVs (blue) of compounds **1a**, **2b**, and **3** recorded in 0.20 M Bu_4N/THF solution.

Table 1, along with that of $Ru_2(ap)_4(C{\equiv}CSi^iPr_3)$[33] for comparison. Similar to the previously reported $Ru_2(Xap)_4(C{\equiv}CR)$ type compounds, compounds **1** and **2** display rich redox chemistry: a reversible one-electron oxidation (**A**), a reversible one-electron reduction (**B**) and an irreversible one-electron reduction (**C**), all of which are Ru_2-based (Scheme 3).[31] Close examination revealed that there is only a slight cathodic shift in the oxidation couple (**A**) and virtually no change in the first reduction couple (**B**) for compounds **1** and **2** from that of $Ru_2(ap)_4(C{\equiv}CSi^iPr_3)$, indicating that the *gem*-DEE ligands are slightly better donors than simple acetylides. It is clear from Table 1 that the electrode potentials for a given couple are identical within experimental errors between $Ru_2(ap)_4$-based (**a**) and $Ru_2(DiMeoap)_4$-based (**b**) compounds, reflecting the equal donor strengths of *ap* and DiMeo*ap* ligands.[13] Since both the oxidation (**A**) and first reduction (**B**) couples are reversible with accurately determined $E_{1/2}$ corresponding to the energies required to remove and add an electron to the HOMO and LUMO, respectively, the electrochemical HOMO−LUMO gap (E_g) of the solvated species can be calculated using the following relationship: E_g = E(LUMO) − E(HOMO) = $E_{1/2}$(**A**) − $E_{1/2}$(**B**). The electro-

DOI: 10.1021/acs.inorgchem.5b01315
Inorg. Chem. 2015, 54, 7645−7652

Table 1. Electrochemical Potentials (V, vs. Ag/AgCl) of Mono-*gem*-DEE Compounds Reported Herein with $Ru_2(ap)_4(C_2Si^iPr_3)(-C_2TIPS)$ for Comparison[33]

compd	$E_{1/2}$(A)	$E_{1/2}$(B)	E_{pc}(C)	E_g (V)	E_{op} (eV)[c]
-C_2TIPS	0.466	−0.877	−2.153[a]	1.343	1.660
1a	0.440	−0.864	−2.088[b]	1.304	1.651
1b	0.438	−0.863	−2.084[a]	1.301	1.644
2a	0.426	−0.872	−2.025[a]	1.298	1.604
2b	0.425	−0.870	−2.044[b]	1.295	1.598
3	0.434 (**A2**)	−0.925 (**B1**)			
	0.370 (**A1**)	−1.082 (**B2**)			

[a] *Quasi*-reversible couple. [b] Irreversible couple, E_{pc} reported. [c] $E_{op} = 10^7/(8065.5\lambda_{max(HOMO-LUMO)})$.

Scheme 3. Assignment of redox couples observed for compounds 1/2 (top) and 3

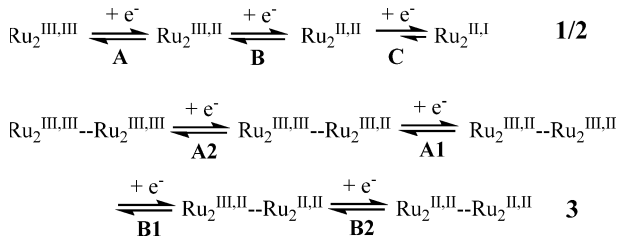

chemical HOMO−LUMO gaps as well as the optical gaps (E_{op} calculated from the longest λ_{max} values) are included in Table 1, and both gaps are within a narrow range of 1.3−1.7 eV, giving promise to these compounds as the starting point for organometallic molecular wires based on cross-conjugated ligands.

The voltammetric behavior of **3** is of particular interest to us, especially when compared with those of compounds **1** and **2**. As clearly shown in Figure 2, compound **3** displays four one-electron couples: a pair of overlapping but resolved oxidations (**A1** and **A2**) at potentials close to that of **A**, and a pair of clearly separated reductions (**B1** and **B2**) at potentials close to that of **B**, which are all Ru_2-based (Scheme 3). The pairwise feature of the $1e^-$ couples is indicative of *possible* electronic coupling between the two Ru_2 termini across the bridging *gem*-DEE, as was previously shown for $[Ru_2(ap)_4]_2(\mu\text{-}C_{2n})$ compounds (n = 1 − 10),[11,13] with the potential splitting within each pair being proportional to the Ru_2−Ru_2 coupling strength.[38] It is worth mentioning that the potential splitting between the oxidative pair (64 mV) is significantly smaller than the splitting between the reductive pair (157 mV). Among limited examples of cross-conjugated/linear oligoyn-diyl pairs, [Ru]-(μ-C≡CC(=C(CN)$_2$)C≡C)-[Ru] ([Ru] = Cp*Ru(dppe)) exhibits pairwise $1e^-$ oxidations with a $\Delta E_{1/2}$ of 200 mV, while [Ru]-(μ-C_4)-[Ru] has a $\Delta E_{1/2}$ = 650 mV, revealing a significant attenuation by the cross-conjugated bridge.[24] The $\Delta E_{1/2}$ for the pairwise Fc oxidations in Fc-(μ-C≡CC(=CBr_2)C≡C)-Fc is about 30 mV, and that of Fc-(μ-C_6)-Fc is about 60 mV.[39] Hence, it is interesting to note that the $\Delta E_{1/2}$s for **3** are comparable to those for $[Ru_2(ap)_4]_2(\mu$-*E*-DEE) (60 mV for oxidations, 220 mV for reductions; *E*-DEE = *E*-hex-3-ene-1,5-diyne and linearly conjugated).[12] Clearly, the attenuation effect of *gem*-DEE exists in the $Ru_2(ap)_4$ system, albeit the decreases in $\Delta E_{1/2}$s are not as drastic as that with the Cp*Ru(dppe) capping group.

Electronic Spectroscopy. All $Ru_2(Xap)_4$ mono-*gem*-DEE compounds are deeply colored and display two absorptions in the visible region in their vis−near-IR (visible−near-infrared) spectra, as shown in Figure 3. Compound **1a** has two intense absorptions centered at 751 and 474 nm, which are comparable

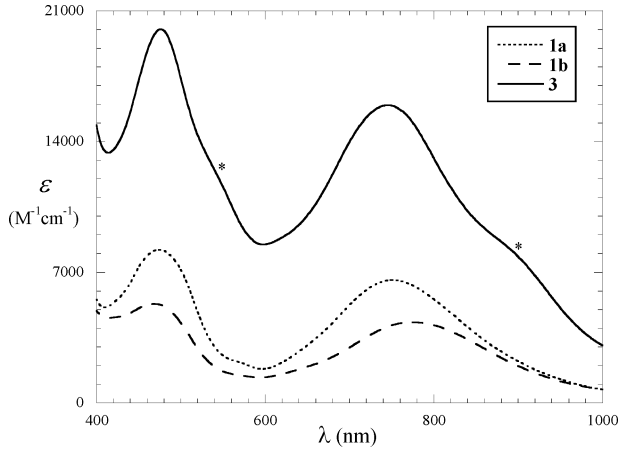

Figure 3. Vis−near-IR spectra of compounds **1a**, **1b**, and **3** in THF solutions.

to those of both $Ru_2(ap)_4Cl$[40] and other $Ru_2(ap)_4$(C≡CY) type compounds.[28,31−33] Compound **1b** has two less intense absorptions centered at 776 and 468 nm.[34] The low-energy absorption can be attributed to the dipole-allowed π(Ru−N)/δ(Ru−Ru) to $\pi^*\delta^*$(Ru−Ru) charge transfer transition, which exhibits a large extinction coefficient ($\varepsilon \sim 6{,}000\ M^{-1}\ cm^{-1}$) due to a significant contribution of N-based π type orbitals to the δ^* orbital. The higher energy and more intense absorption ($\varepsilon \sim 8{,}000\ M^{-1}\ cm^{-1}$) is likely due to the dipole-allowed LMCT transition from the π(N) orbital to the $\pi^*\delta^*$(Ru−Ru), which has a significant contribution from the π^*(C≡C) of the axial *gem*-DEE ligands as previously noted for other $Ru_2(Xap)_4$(C≡CY) type compounds.[29,34] It is also noteworthy that the lowest energy transition optical energy gaps (E_{op}) for these new $Ru_2(Xap)_4$ mono-*gem*-DEE compounds (*ca.* 1.65 eV) are larger than their electrochemical energy gaps (*ca.* 1.32 eV), which is likely due to the open-shell nature of $Ru_2(Xap)_4$ compounds.

Dimeric compound **3** is an intense absorber in the vis−near-IR region, and its spectrum is also shown in Figure 3, which features intense peaks at 746 and 476 nm and shoulders at *ca.* 900 and 540 nm (indicated by asterisks (*)). The positions of intense peaks correspond well with those observed for compounds **1** and **2** and are likely originated from the same types of electronic transitions. The appearance of the shoulders adjacent to the intense peaks resembles the feature observed for the $[Ru_2(Xap)_4]_2(\mu\text{-}C_{2n})$ type compounds,[11,13] which is attributed to the electronic coupling between two Ru_2 termini across the linear oligoyn-diyl bridge. The shoulders are much

DOI: 10.1021/acs.inorgchem.5b01315
Inorg. Chem. 2015, 54, 7645−7652

less discernible in **3** though, reflecting a significantly weakened $Ru_2 - Ru_2$ coupling mediated by the *gem*-DEE bridge.

Spectroelectrochemistry. The vis−near-IR spectroelectrochemical reduction of the monomer compound **1a** in THF is shown in Figure 4. Upon reduction (Figure 4a), the only

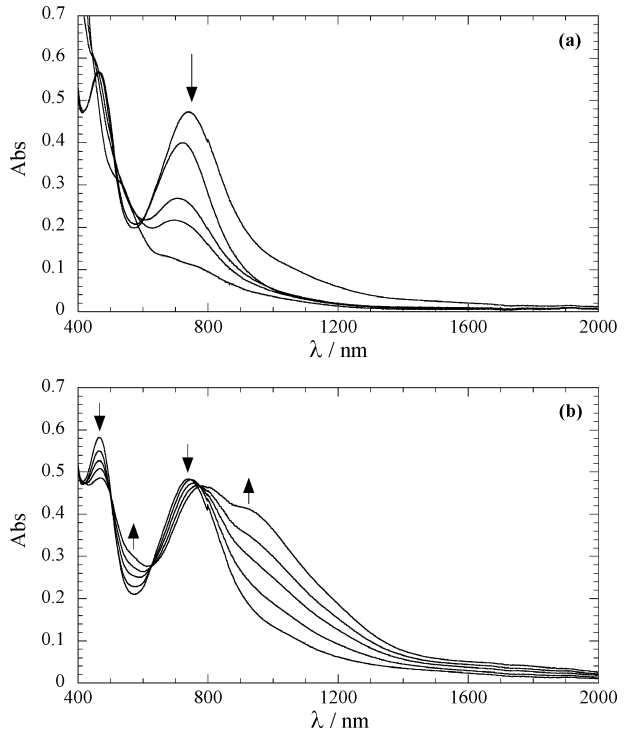

Figure 4. Spectroelectrochemical (a) reduction and (b) oxidation of **1a** in THF, 0.1 M TBAH.

significant change is a loss of intensity of the low-energy band at 751 nm consistent with this band's assignment as a π(Ru−N)/δ(Ru−Ru) to $\pi^*\delta^*$(Ru−Ru) charge transfer transition. Oxidation of **1a** (Figure 4b) results in a new band appearing as a shoulder at *ca.* 940 nm which is likely also a charge transfer transition, though the rises and falls of the peaks are not as pronounced as those observed for simple alkynyl compounds.[41]

Figure 5 shows the spectroelectrochemical reduction of the dimer compound **3**. For Figure 5a, the one-electron reduction of **3** causes a general increase in intensity of the absorption bands and also the appearance of a weak near-IR absorption at wavelengths greater than 1000 nm. The latter might have been considered to be a weak intervalence transition, however addition of a second electron (Figure 5b) results in the loss of the 742 nm band and little change in the absorption intensity at wavelengths greater than 1000 nm. Thus, no absorption in the near-IR, unique to the mixed-valence state $\mathbf{3}^-$, was observed. Spectroelectrochemical oxidation of **3** is provided in the Supporting Information (Figure S1), where the most significant change upon one-electron oxidation to $\mathbf{3}^+$ is the growth of a new transition centered at 1100 nm. Further oxidation to $\mathbf{3}^{2+}$ blue shifts the absorption of the 1100 nm band to 960 nm and increases the band intensity. The spectra of $\mathbf{3}^{2+}$ (Supporting Information Figure S1b) and $\mathbf{3}^{2-}$ (Figure 5b) closely resemble those of the monomer complexes $\mathbf{1a}^+$ (Figure 4b) and $\mathbf{1a}^-$ (Figure 4a), respectively, as expected.

Density Functional Theory Study. In order to gain further insight into the nature of the electronic coupling within

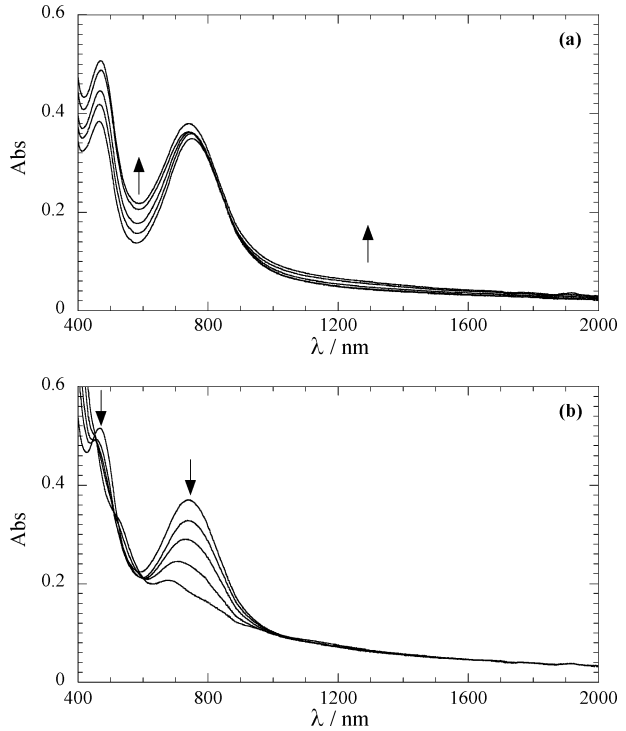

Figure 5. Spectroelectrochemical (a) one-electron reduction and (b) two-electron reduction of **3** in THF, 0.1 M TBAH.

compound **3**, the molecular orbitals of model compound **3′** were computed using spin-unrestricted DFT.[42] The initial geometry of **3′** was based on the X-ray structure of monomeric compound **1b** with a second $Ru_2(ap)_4$ unit of identical metrical parameters replacing the terminal -H of the *gem*-DEE ligand. The geometry of **3′** (Tables S1 and S2 and Figure S2 in the Supporting Information) was optimized using the unrestricted B3LYP functional and was found to be a stationary point by frequency analysis. The six SOMOs of **3′** are shown in Figure 6.

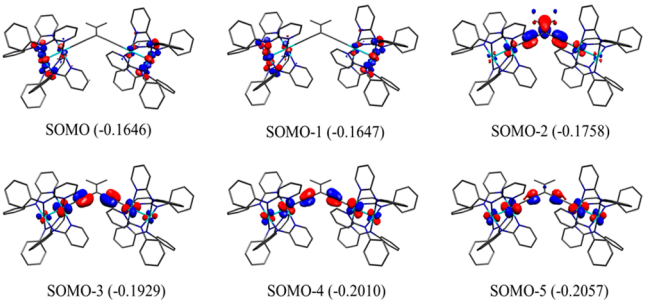

Figure 6. Singly occupied molecular orbitals (SOMOs) and their energies (in hartree) of **3′**. Hydrogen atoms have been omitted for clarity.

$Ru_2(Xap)_4$ monoalkynyl compounds generally have three unpaired electrons with an ground state electron configuration of $\sigma^2\pi^4\delta^2\pi^{*2}\delta^*$.[41] Similar configurations have been shown for oligoyn-diyl bridged species $[Ru_2(Xap)_4]_2(\mu\text{-}C_{2n})$.[11,13] The SOMO and SOMO-1 are $\delta^*(Ru_2)$ in character and are primarily composed of the Ru d_{xy} orbitals, which are orthogonal to the π(C≡C) orbitals of the bridging *gem*-DEE ligand. The SOMO and SOMO-1 are nearly degenerate and can each be considered a localized electron within the Ru_2(II,III) fragment as a result of the weak interaction between the two Ru_2 centers.

DOI: 10.1021/acs.inorgchem.5b01315
Inorg. Chem. 2015, 54, 7645−7652

The SOMO-2 is composed of $\pi^*(Ru_2)$ orbitals and out-of-plane π(*gem*-DEE) orbitals, where the filled−filled type antibonding interactions between $d\pi$(Ru) and π(C≡C) are prominent. Though composed of $\pi^*(Ru_2)$ orbitals and out-of-plane π(*gem*-DEE) orbitals as well, the SOMO-4 is distinguished from SOMO-2 with the two π(C≡C) orbitals being out-of-phase, and contains no contribution from the π(ethene) orbital. The SOMO-3 and SOMO-5 are composed of $\pi^*(Ru_2)$ orbitals and in-plane π(*gem*-DEE) orbitals. In particular, the two in-plane π(C≡C) orbitals in SOMO-5 are in phase and have constructive bonding interaction even though two acetylene bonds are not conjugated, as noted in an earlier DFT study of the H-*gem*-DEE ligand.[43] It is conceivable that the electronic coupling between Ru_2 termini is mostly facilitated by SOMO-5, while SOMO-2/3/4 may also contribute. In general, the compositions of the SOMOs that span the bridging molecule are in distinctive contrast to the SOMOs found for $[Ru_2(Xap)_4]_2(\mu\text{-}C_{2n})$, where extensive involvement of π(C≡C) orbitals across the entire oligoyndiyl bridge is clear from SOMO-2 to SOMO-5.[11,13]

CONCLUSION

Several $Ru_2(Xap)_4$(*gem*-DEE) type compounds and dimeric $[Ru_2(ap)_4]_2$(*μ-gem*-DEE) have been prepared and characterized with X-ray diffraction, voltammetric, and spectroscopic techniques. The *gem*-DEE containing $Ru_2(Xap)_4$ compounds bear spectroscopic and voltammetric characteristics similar to those of $Ru_2(ap)_4(C{\equiv}CY)$ compounds. Interestingly, the bridged dimer $[Ru_2(ap)_4]_2$(*μ-gem*-DEE) displays pairwise $1e^-$ oxidations and reductions that were commonly observed for highly conjugated $[Ru_2(ap)_4]_2(\mu\text{-}C_{2n})$ (n = 1−8). However, the spectroelectrochemical study of **3** did not yield any discernible IVCT band(s) for either $\mathbf{3}^{+1}$ or $\mathbf{3}^{-1}$, indicating a weak delocalization in these mixed-valent ions. DFT calculations of **3** revealed that, among six SOMOs, there is only one (SOMO-5) with significant and contiguous $d\pi$−π(C≡C) contribution along the Ru_2-*μ-gem*-DEE-Ru_2 linkage, corroborating the aforementioned weak delocalization.

EXPERIMENTAL SECTION

General Methods. The *gem*-DEE ligands,[44] $Ru_2(ap)_4Cl$[31] and $Ru_2(DiMeOap)_4Cl$[34] were prepared according to the literature procedures. Tetrahydrofuran was freshly distilled over sodium/benzophenone, while hexanes were freshly distilled over CaH_2 prior to use. All reactions were performed under dry N_2 atmosphere implementing standard Schlenk procedures unless otherwise noted. Vis−near-IR spectra were obtained with a JASCO V-670 spectrophotometer in THF solutions. FT-IR spectra were measured on neat samples with a JASCO FT/IR-6300 spectrometer. Nano-ESI-MS (nESI) spectra were performed on a QqQ tandem mass spectrometer in CH_2Cl_2 (QTRAP4000; Applied Biosystems/MDS Sciex, Concord, ON, Canada). HR-nESI-MS spectra were performed on a modified QqTOF tandem mass spectrometer in CH_2Cl_2 (QSTAR XL; Applied Biosystems/MDS Sciex). Masses were calculated by isotopic distribution utilizing Analyst 1.6 software (Applied Biosystems/MDS Sciex). Magnetic susceptibility measurements were conducted using a Johnson Matthey Mark-I magnetic susceptibility balance. Cyclic and differential voltammograms were recorded in 0.2 M $(n\text{-}Bu)_4NPF_6$ solution (THF, N_2-degassed) on a CHI620A voltammetric analyzer with a glassy carbon working electrode (diameter = 2 mm), a Pt-wire auxiliary electrode, and a Ag/AgCl reference electrode. The concentration of Ru_2-species is always 1.0 mM. The ferrocenium/ferrocene couple was observed at 0.570 V (vs Ag/AgCl) at the noted experimental conditions.

General Method for the Preparation of Mono-Ru_2 Silyl Capped *gem*-DEE Compounds (1a and 1b). A Schlenk flask (100 mL) was charged with 1 equiv of $Ru_2(ap)_4Cl$ (for **1a**) or $Ru_2(DiMeOap)_4Cl$ (for **1b**) and freshly distilled, degassed THF. A separate Schlenk tube (25 mL) was charged with 1.5 equiv of the appropriate Y-*gem*-DEE and 5 mL of THF, to which was added 1.65 equiv (1.1 equiv of Y-*gem*-DEE ligand) of 2.5 M *n*-BuLi at −100 °C, and the mixture was allowed to warm to room temperature in 1 h. The *in situ* formed Li-*gem*-DEE-Y was transferred via cannula to the stirring solution of Ru_2, resulting in an instantaneous change of the color from green to brown. The reaction was allowed to stir at room temperature overnight. After the removal of solvents, the residue was dissolved in EtOAc/hexanes (1:4) and filtered through a silica gel plug. Further recrystallization from THF/MeOH at −18 °C provided desired products.

*$Ru_2(ap)_4(^iPr_3Si$-gem-DEE) (**1a**).* Starting from 0.39 g of $Ru_2(ap)_4Cl$ (0.42 mmol), 0.44 g of **1a** (0.39 mmol, 93%) was obtained as a brown solid. Data for **1a**: R_f = 0.66 (1:1:10 EtOAc/Et_3N/hexanes). nESI-MS (m/z, based on ^{101}Ru): 1139.3, corresponding to $[M + H]^+$. HR-nESI-MS (m/z, based on ^{101}Ru): 1139.311, corresponding to $[M + H]^+$ ($C_{61}H_{63}N_8Si_1Ru_2$; calcd, 1139.305). Vis−near-IR (λ_{max}, nm (ε, M^{-1} cm^{-1})): 751 (6,600), 474 (8190). FT-IR (neat, ν (cm^{-1})): 2143 (-C≡C−Si^iPr_3) and 2035 (Ru−C≡C−). Cyclic voltammogram [$E_{1/2}$/V, ΔE_p/V, $i_{backward}/i_{forward}$]: **A**, 0.440, 0.034, 0.980; **B**, −0.864, 0.026, 1.000; E_{pc}(**C**), −2.088. μ_{eff} = 3.73 μ_B.

$Ru_2(DiMeOap)_4(^iPr_3Si$-*gem*-DEE) (1b). Starting from 0.30 g of $Ru_2(DiMeOap)_4Cl$ (0.26 mmol), 0.27 g of **1b** (0.20 mmol, 77%) was isolated as a brown solid. Data for **1b**: R_f = 0.35 (1:1:3 THF/Et_3N/hexanes). nESI-MS (m/z, based on ^{101}Ru): 1380, corresponding to $[M + H]^+$. HR-nESI-MS (m/z, based on ^{101}Ru): 1379.386, corresponding to $[M + H]^+$ ($C_{69}H_{79}O_8N_8Si_1Ru_2$; calcd, 1379.390). Vis−near-IR (λ_{max}, nm (ε, M^{-1} cm^{-1})): 776 (4340), 468 (5320). FT-IR (neat, ν (cm^{-1})): 2141 (-C≡C−Si^iPr_3) and 2033 (Ru−C≡C-). Cyclic voltammogram [$E_{1/2}$/V, ΔE_p/V, $i_{backward}/i_{forward}$]: **A**, 0.426, 0.032, 0.986; **B**, −0.872, 0.034, 1.000; E_{pc}(**C**), −2.025. μ_{eff} = 3.67 μ_B.

$Ru_2(ap)_4$(H-*gem*-DEE) (2a). Compound **1a** (0.255 g, 0.224 mmol) was treated with a catalytic amount of $(n\text{-}Bu)_4NF$, and the reaction mixture was filtered through silica and recrystallized from THF/pentane to yield 0.187 g of **2a** (85%) as a brown crystalline solid. Data for **2a**: R_f = 0.36 (1:1:10 EtOAc/Et_3N/hexanes). nESI-MS (m/z, based on ^{101}Ru): 983.6, corresponding to $[M + H]^+$. HR-nESI-MS (m/z, based on ^{101}Ru): 983.169, corresponding to $[M + H]^+$ ($C_{52}H_{43}N_8Ru_2$, calc. 983.171). Vis−near-IR (λ_{max}, nm (ε, M^{-1} cm^{-1})): 751 (5950), 479 (7590). FT-IR (neat, ν (cm^{-1})): 2094 (-C≡C−H) and 2023 (Ru−C≡C−). Cyclic voltammogram [$E_{1/2}$/V, ΔE_p/V, $i_{backward}/i_{forward}$]: **A**, 0.438, 0.033, 0.872; **B**, −0.863, 0.031, 1.000; E_{pc}(**C**), −2.084. μ_{eff} = 3.80 μ_B. Elemental analysis calcd (%) for $C_{52}H_{43}N_8Ru_2\cdot(1/2)H_2O$ (**1b**·0.5H_2O): C 63.02, H 4.46, N 11.31; found: C 62.74, H 4.32, N 11.28.

$Ru_2(DiMeOap)_4$(H-*gem*-DEE) (2b). Compound **1b** (0.200 g, 0.145 mmol was treated with a catalytic amount of $(n\text{-}Bu)_4NF$, and the reaction mixture was filtered through silica and recrystallized from THF/pentane to yield 0.132 g of **2b** (75%) as a brown microcrystalline solid. Data for **2b**: R_f = 0.19 (1:1:3 THF/Et_3N/hexanes). nESI-MS (m/z, based on ^{101}Ru): 1223, corresponding to $[M + H]^+$. HR-nESI-MS (m/z, based on ^{101}Ru): 1223.251, corresponding to $[M + H]^+$ ($C_{60}H_{59}O_8N_8Ru_2$; calcd, 1223.256). Vis−near-IR (λ_{max}, nm (ε, M^{-1} cm^{-1})): 777 (4030), 481 (5400). FT-IR (neat, ν (cm^{-1})): 2108 (-C≡C−H) and 2027 (Ru−C≡C-). Cyclic voltammogram [$E_{1/2}$/V, ΔE_p/V, $i_{backward}/i_{forward}$]: **A**, 0.425, 0.031, 0.913; **B**, −0.870, 0.031, 0.916; E_{pc}(**C**), −2.044. μ_{eff} = 3.72 μ_B.

$[Ru_2(ap)_4]_2$(*μ-gem*-DEE) (3). *Method A.* In a 100 mL, three-neck round-bottom flask fitted with an addition tube containing 2 equiv of solid $Ru_2(ap)_4Cl$ (0.40 g, 0.44 mmol), was added 1 equiv of *gem*-DEE (0.02 mL, 0.25 mmol) and 35 mL of THF. Following three freeze−pump−thaw cycles, 2.2 equiv of *n*-BuLi (0.20 mL, 0.49 mmol) was added dropwise while allowing the flask to warm to 0 °C. The reaction mixture was stirred for 1 h at 0 °C under N_2 prior to the addition of $Ru_2(ap)_4Cl$ by turning the addition tube, which changed the solution color from light yellow to brownish-purple. The reaction was stirred

DOI: 10.1021/acs.inorgchem.5b01315
Inorg. Chem. 2015, 54, 7645−7652

overnight, and hexanes was added at the end. The dark precipitate was collected under argon and rinsed with copious amounts of hexanes. The collected solid was recrystallized in toluene/hexanes at −30 °C to yield 0.14 g of **3** (0.08 mmol, 32% based on *gem*-DEE) as a purplish-brown solid.

Method B. To a 100 mL, three-neck round-bottom flask fitted with an addition tube containing 0.98 equiv of solid $Ru_2(ap)_4Cl$ (0.18 g, 0.20 mmol) was added 1 equiv of $Ru_2(ap)_4$(H-*gem*-DEE) (**1b**) (0.20 g, 0.20 mmol) and THF (25 mL). Following three freeze−pump−thaw cycles, 1.1 equiv of *n*-BuLi (0.09 mL, 0.22 mmol) was added dropwise at −78 °C (dry ice/acetone). The reaction was stirred for 1 h at −78 °C prior to the addition of solid $Ru_2(ap)_4Cl$ with the color of the solution changing to brownish-purple. The reaction was stirred for another hour at −78 °C and then at room temperature overnight. The same workup as that of method A resulted in 0.190 g of **3** (50% based on **1b**).

Data for **3**: R_f = baseline (1:1:3 THF/Et_3N/hexanes). nESI-MS (*m*/*z*, based on ^{101}Ru): 1861, corresponding to $[M + H]^+$. Vis−near-IR (λ_{max}, nm (ε, M^{-1} cm^{-1})): 880 (sh), 746 (16,000), 540 (sh), 476 (20,000). Cyclic voltammogram [$E_{1/2}$/V, ΔE_p/V, $i_{backward}/i_{forward}$]: E_{pa}(**A2**), 0.434; E_{pa}(**A1**), 0.370; **B1**, −0.925, 0.029, 0.656; **B2**, −1.082, 0.037, 1.000. μ_{eff} = 6.39 μ_B (4.52 μ_B/Ru_2). Elem. Anal. Calcd (%) for $C_{96}H_{78}N_{16}Ru_4 \cdot H_2O$ (**3**·H_2O): C 61.44, H 4.29, N 11.93; found: C 61.11, H 3.89, N 11.77.

Spectroelectrochemistry of 3. An OTTLE cell was used to perform the spectroelectrochemistry at ambient temperatures.[45] The cell had interior dimensions of roughly 1 × 2 cm with a path length of 0.2 mm and was fitted with a Ag/AgCl reference electrode and ITO (indium−tin oxide) coated glass for the working and counter electrodes. All of the spectroelectrochemical transformations showed good reversibility (greater than 95% recovery of original complex spectrum).

Computational Details. DFT computations were performed using the unrestricted B3LYP functional[46] as implemented in Gaussian 03[42] H atoms were represented by the 3-21G basis set;[47] C and N were represented by the 6-31G* basis set,[48] and Ru was represented by the LANL2DZ basis set and effective core potential (ECP).[49] The structure was optimized without any geometric constraints. The initial SCF convergence criteria was set to 1×10^{-7} Eh. The wave function was found to be stable, and frequency analysis showed the structure is a minimum on the potential energy surface (no negative frequencies). Following initial optimization, the structure was reoptimized using a convergence criteria of 1×10^{-8} Eh without use of integral symmetry. The reoptimization found a structure with the same energy and metrical parameters. Population analysis was performed to obtain the molecular orbitals which were rendered using the MOLEKEL visualization package.[50]

X-ray Structural Analysis of 2a. Single crystals of compound **2a** suitable for X-ray structural determination were grown via slow cooling of a THF/pentane solution under N_2 at −18 °C; pentane is present in single crystal. X-ray diffraction data for **2a** were collected on a Rigaku Rapid II image plate diffractometer using Cu Kα at 150 K, and the structure was solved using the structure solution program PATTY in DIRDIF99,[51] and refined using SHELX-07.[52] Crystal Data of **2a**: $C_{57}H_{55}N_8Ru_2$, fw = 1054.27, $P\bar{1}$, a = 9.980(2), b = 13.587(2), c = 18.825(3) Å, α = 100.92(1)°, β = 93.27(1)°, γ = 93.84(1)°, V = 2494.3(7) $Å^3$, Z = 2, D_{calcd} = 1.404 g cm^{-3}, R1 = 0.082, and wR2 = 0.226.

■ ASSOCIATED CONTENT

Supporting Information

Spectroelectrochemical oxidations of **3**, optimized structure of **3′**, details of DFT calculations of **3′**, and X-ray crystallographic files in CIF format for the structure determination of compound **2a**. The Supporting Information is available free of charge on the ACS Publications website at DOI: 10.1021/acs.inorgchem.5b01315.

■ AUTHOR INFORMATION

Corresponding Author

*E-mail: tren@purdue.edu.

Notes

The authors declare no competing financial interest.

■ ACKNOWLEDGMENTS

We gratefully acknowledge the financial support from the National Science Foundation (Grant CHE 1362214) to T.R. and the Natural Sciences and Engineering Research Council of Canada to R.J.C.

■ REFERENCES

(1) (a) Bruce, M. I.; Low, P. J. Transition Metal Complexes Containing All-Carbon Ligands. *Advances in Organometallic Chemistry*; Elsevier: Amsterdam, 2004; Vol. *50*, pp 179−444. (b) Zhang, X.-Y.; Zheng, Q.; Qian, C.-X.; Zuo, J.-L. *Chin. J. Inorg. Chem.* **2011**, *27*, 1451−1464.

(2) (a) Costuas, K.; Rigaut, S. *Dalton Trans.* **2011**, *40*, 5643−5658. (b) Halet, J. F.; Lapinte, C. *Coord. Chem. Rev.* **2013**, *257*, 1584−1613.

(3) Whittall, I. R.; McDonagh, A. M.; Humphrey, M. G.; Samoc, M. *Adv. Organomet. Chem.* **1998**, *42*, 291−362.

(4) (a) Szafert, S.; Gladysz, J. A. *Chem. Rev.* **2003**, *103*, 4175−4206. (b) Ren, T. *Organometallics* **2005**, *24*, 4854−4870.

(5) (a) Brady, M.; Weng, W.; Zhou, Y.; Seyler, J. W.; Amoroso, A. J.; Arif, A. M.; Bohme, M.; Frenking, G.; Gladysz, J. A. *J. Am. Chem. Soc.* **1997**, *119*, 775−788. (b) Dembinski, R.; Bartik, T. s.; Bartik, B.; Jaeger, M.; Gladysz, J. A. *J. Am. Chem. Soc.* **2000**, *122*, 810−822. (c) Zhou, Y.; Seyler, J. W.; Weng, W.; Arif, A. M.; Gladysz, J. A. *J. Am. Chem. Soc.* **1993**, *115*, 8509−8510.

(6) (a) Le Narvor, N.; Toupet, L.; Lapinte, C. *J. Am. Chem. Soc.* **1995**, *117*, 7129−7138. (b) Lissel, F.; Fox, T.; Blacque, O.; Polit, W.; Winter, R. F.; Venkatesan, K.; Berke, H. *J. Am. Chem. Soc.* **2013**, *135*, 4051−4060.

(7) (a) Bruce, M. I.; Low, P. J.; Costuas, K.; Halet, J.-F.; Best, S. P.; Heath, G. A. *J. Am. Chem. Soc.* **2000**, *122*, 1949−1962. (b) Olivier, C.; Costuas, K.; Choua, S.; Maurel, V.; Turek, P.; Saillard, J.-Y.; Touchard, D.; Rigaut, S. *J. Am. Chem. Soc.* **2010**, *132*, 5638−5651. (c) Bruce, M. I.; Cole, M. L.; Ellis, B. G.; Gaudio, M.; Nicholson, B. K.; Parker, C. R.; Skelton, B. W.; White, A. H. *Polyhedron* **2015**, *86*, 43−56.

(8) (a) Zheng, Q.; Gladysz, J. A. *J. Am. Chem. Soc.* **2005**, *127*, 10508−10509. (b) Stahl, J.; Mohr, W.; de Quadras, L.; Peters, T. B.; Bohling, J. C.; Martín-Alvarez, J. M.; Owen, G. R.; Hampel, F.; Gladysz, J. A. *J. Am. Chem. Soc.* **2007**, *129*, 8282−8295. (c) Baranová, Z.; Amini, H.; Bhuvanesh, N.; Gladysz, J. A. *Organometallics* **2014**, *33*, 6746−6749.

(9) Ren, T.; Zou, G.; Alvarez, J. C. *Chem. Commun.* **2000**, 1197−1198.

(10) (a) Wong, K.-T.; Lehn, J.-M.; Peng, S.-M.; Lee, G.-H. *Chem. Commun.* **2000**, 2259−2260. (b) Ying, J.-W.; Liu, I. P.-C.; Xi, B.; Song, Y.; Campana, C.; Zuo, J.-L.; Ren, T. *Angew. Chem., Int. Ed.* **2010**, *49*, 954−957. (c) Ying, J.-W.; Cao, Z.; Campana, C.; Song, Y.; Zuo, J.-L.; Tyler, S. F.; Ren, T. *Polyhedron* **2015**, *86*, 76−80.

(11) Xu, G.-L.; Zou, G.; Ni, Y.-H.; DeRosa, M. C.; Crutchley, R. J.; Ren, T. *J. Am. Chem. Soc.* **2003**, *125*, 10057−10065.

(12) Shi, Y.; Yee, G. T.; Wang, G.; Ren, T. *J. Am. Chem. Soc.* **2004**, *126*, 10552−10553.

(13) (a) Xi, B.; Liu, I. P.-C.; Xu, G.-L.; Choudhuri, M. M. R.; DeRosa, M. C.; Crutchley, R. J.; Ren, T. *J. Am. Chem. Soc.* **2011**, *133*, 15094−15104. (b) Cao, Z.; Xi, B.; Jodoin, D. S.; Zhang, L.; Cummings, S. P.; Gao, Y.; Tyler, S. F.; Fanwick, P. E.; Crutchley, R. J.; Ren, T. *J. Am. Chem. Soc.* **2014**, *136*, 12174−12183.

(14) (a) Liu, S. H.; Xia, H.; Wen, T. B.; Zhou, Z.; Jia, G. *Organometallics* **2003**, *22*, 737−743. (b) Liu, S. H.; Hu, Q. Y.; Xue, P.; Wen, T. B.; Williams, I. D.; Jia, G. C. *Organometallics* **2005**, *24*, 769−772. (c) Yuan, P.; Wu, X. H.; Yu, G. A.; Du, D.; Liu, S. H. *J. Organomet. Chem.* **2007**, *692*, 3588−3592.

DOI: 10.1021/acs.inorgchem.5b01315
Inorg. Chem. 2015, 54, 7645−7652

(15) (a) Etzenhouser, B. A.; Cavanaugh, M. D.; Spurgeon, H. N.; Sponsler, M. B. *J. Am. Chem. Soc.* **1994**, *116*, 2221−2222. (b) Chung, M.-C.; Gu, X.; Etzenhouser, B. A.; Spuches, A. M.; Rye, P. T.; Seetharaman, S. K.; Rose, D. J.; Zubieta, J.; Sponsler, M. B. *Organometallics* **2003**, *22*, 3485−3494.
(16) Nielsen, M. B.; Diederich, F. *Chem. Rev.* **2005**, *105*, 1837−1868.
(17) Gholami, M.; Tykwinski, R. R. *Chem. Rev.* **2006**, *106*, 4997−5027.
(18) Zucchero, A. J.; McGrier, P. L.; Bunz, U. H. F. *Acc. Chem. Res.* **2010**, *43*, 397−408.
(19) Phelan, N. F.; Orchin, M. *J. Chem. Educ.* **1968**, *45*, 633.
(20) Diederich, F.; Kivala, M. *Adv. Mater.* **2010**, *22*, 803−812.
(21) Tykwinski, R. R.; Zhao, Y. M. *Synlett* **2002**, 1939−1953.
(22) (a) Opsitnick, E.; Lee, D. *Chem. - Eur. J.* **2007**, *13*, 7040−7049. (b) Kivala, M.; Diederich, F. *Acc. Chem. Res.* **2009**, *42*, 235−248. (c) Guthrie, D. A.; Tovar, J. D. *Chem. - Eur. J.* **2009**, *15*, 5176−5185.
(23) (a) Campbell, K.; McDonald, R.; Ferguson, M. J.; Tykwinski, R. R. *Organometallics* **2003**, *22*, 1353−1355. (b) Campbell, K.; McDonald, R.; Ferguson, M. J.; Tykwinski, R. R. *J. Organomet. Chem.* **2003**, *683*, 379−387. (c) Campbell, K.; Johnson, C. A.; McDonald, R.; Ferguson, M. J.; Haley, M. M.; Tykwinski, R. R. *Angew. Chem., Int. Ed.* **2004**, *43*, 5967−5971.
(24) Bruce, M. I.; Burgun, A.; Fox, M. A.; Jevric, M.; Low, P. J.; Nicholson, B. K.; Parker, C. R.; Skelton, B. W.; White, A. H.; Zaitseva, N. N. *Organometallics* **2013**, *32*, 3286−3299.
(25) (a) Forrest, W. P.; Cao, Z.; Fanwick, P. E.; Hassell, K. M.; Ren, T. *Organometallics* **2011**, *30*, 2075−2078. (b) Forrest, W. P.; Cao, Z.; Hassell, K. M.; Prentice, B. M.; Fanwick, P. E.; Ren, T. *Inorg. Chem.* **2012**, *51*, 3261−3269.
(26) Forrest, W. P.; Cao, Z.; Hambrick, R.; Prentice, B. M.; Fanwick, P. E.; Wagenknecht, P. S.; Ren, T. *Eur. J. Inorg. Chem.* **2012**, *2012*, 5616−5620.
(27) Cao, Z.; Fanwick, P. E.; Forrest, W. P.; Gao, Y.; Ren, T. *Organometallics* **2013**, *32*, 4684−4689.
(28) Chakravarty, A. R.; Cotton, F. A. *Inorg. Chim. Acta* **1986**, *113*, 19−26.
(29) Li, Y.; Han, B.; Kadish, K. M.; Bear, J. L. *Inorg. Chem.* **1993**, *32*, 4175−4176.
(30) (a) Bear, J. L.; Han, B.; Huang, S.; Kadish, K. M. *Inorg. Chem.* **1996**, *35*, 3012−3021. (b) Bear, J. L.; Li, Y.; Han, B.; Van Caemelbecke, E.; Kadish, K. M. *Inorg. Chem.* **1997**, *36*, 5449−5456. (c) Bear, J. L.; Han, B.; Wu, Z.; Van Caemelbecke, E.; Kadish, K. M. *Inorg. Chem.* **2001**, *40*, 2275−2281. (d) Kadish, K. M.; Phan, T. D.; Giribabu, L.; Van Caemelbecke, E.; Bear, J. L. *Inorg. Chem.* **2003**, *42*, 8663−8673. (e) Kadish, K. M.; Phan, T. D.; Wang, L.-L.; Giribabu, L.; Thuriere, A.; Wellhoff, J.; Huang, S.; Caemelbecke, E. V.; Bear, J. L. *Inorg. Chem.* **2004**, *43*, 4825−4832. (f) Nguyen, M.; Phan, T.; Caemelbecke, E. V.; Kajonkijya, W.; Bear, J. L.; Kadish, K. M. *Inorg. Chem.* **2008**, *47*, 7775−7783. (g) Manowong, M.; Van Caemelbecke, E.; Rodriguez-Morgade, M. S.; Bear, J. L.; Kadish, K. M.; Torres, T. *J. Porphyrins Phthalocyanines* **2014**, *18*, 49−57.
(31) Zou, G.; Alvarez, J. C.; Ren, T. *J. Organomet. Chem.* **2000**, *596*, 152−158.
(32) Xu, G.; Ren, T. *Organometallics* **2001**, *20*, 2400−2404.
(33) Ren, T. *Organometallics* **2002**, *21*, 732−738.
(34) Xi, B.; Xu, G.-L.; Ying, J.-W.; Han, H.-L.; Cordova, A.; Ren, T. *J. Organomet. Chem.* **2008**, *693*, 1656−1663.
(35) Cotton, F. A.; Ren, T. *Inorg. Chem.* **1995**, *34*, 3190−3193.
(36) Jahnke, E.; Tykwinski, R. R. *Chem. Commun.* **2010**, *46*, 3235−3249.
(37) Angaridis, P., Ruthenium Compounds. In *Multiple Bonds between Metal Atoms*, 3rd ed.; Cotton, F. A., Murillo, C. A., Walton, R. A., Eds.; Springer Science and Business Media: New York, 2005.
(38) (a) Crutchley, R. J. *Adv. Inorg. Chem.* **1994**, *41*, 273−325. (b) Creutz, C. Mixed Valence Complexes of d^5−d^6 Metal Centers. *Progress in Inorganic Chemistry: An Appreciation of Henry Taube*; John Wiley & Sons: New York, 1983; Vol. *30*, pp 1−73. (c) Richardson, D. E.; Taube, H. *Inorg. Chem.* **1981**, *20*, 1278−1285. (d) Richardson, D. E.; Taube, H. *Coord. Chem. Rev.* **1984**, *60*, 107−129.
(39) Xu, G.-L.; Xi, B.; Updegraff, J. B.; Protasiewicz, J. D.; Ren, T. *Organometallics* **2006**, *25*, 5213−5215.
(40) Chakravarty, A. R.; Cotton, F. A.; Tocher, D. A. *Inorg. Chem.* **1985**, *24*, 172−177.
(41) Zhang, L.; Xi, B.; Po-Chun Liu, I.; Choudhuri, M. M. R.; Crutchley, R. J.; Updegraff, J. B.; Protasiewicz, J. D.; Ren, T. *Inorg. Chem.* **2009**, *48*, 5187−5194.
(42) Frisch, M. J.; Trucks, G. W.; Schlegel, H. B.; Scuseria, G. E.; Robb, M. A.; Cheeseman, J. R.; Montgomery, J. A., Jr.; Vreven, T.; Kudin, K. N.; Burant, J. C.; Millam, J. M.; Iyengar, S. S.; Tomasi, J.; Barone, V.; Mennucci, B.; Cossi, M.; Scalmani, G.; Rega, N.; Petersson, G. A.; Nakatsuji, H.; Hada, M.; Ehara, M.; Toyota, K.; Fukuda, R.; Hasegawa, J.; Ishida, M.; Nakajima, T.; Honda, Y.; Kitao, O.; Nakai, H.; Klene, M.; Li, X.; Knox, J. E.; Hratchian, H. P.; Cross, J. B.; Bakken, V.; Adamo, C.; Jaramillo, J.; Gomperts, R.; Stratmann, R. E.; Yazyev, O.; Austin, A. J.; Cammi, R.; Pomelli, C.; Ochterski, J. W.; Ayala, P. Y.; Morokuma, K.; Voth, G. A.; Salvador, P.; Dannenberg, J. J.; Zakrzewski, V. G.; Dapprich, S.; Daniels, A. D.; Strain, M. C.; Farkas, O.; Malick, D. K.; Rabuck, A. D.; Raghavachari, K.; Foresman, J. B.; Ortiz, J. V.; Cui, Q.; Baboul, A. G.; Clifford, S.; Cioslowski, J.; Stefanov, B. B.; Liu, G.; Liashenko, A.; Piskorz, P.; Komaromi, I.; Martin, R. L.; Fox, D. J.; Keith, T.; Al-Laham, M. A.; Peng, C. Y.; Nanayakkara, A.; Challacombe, M.; Gill, P. M. W.; Johnson, B.; Chen, W.; Wong, M. W.; Gonzalez, C.; Pople, J. A. *Gaussian 03*, Revision D.02; Gaussian: Wallingford, CT, USA, 2003.
(43) Cao, Z.; Ren, T. *Organometallics* **2011**, *30*, 245−250.
(44) Zhao, Y.; McDonald, R.; Tykwinski, R. R. *J. Org. Chem.* **2002**, *67*, 2805−2812.
(45) Krejcik, M.; Danek, M.; Hartl, F. *J. Electroanal. Chem. Interfacial Electrochem.* **1991**, *317*, 179−187.
(46) (a) Becke, A. D. *J. Chem. Phys.* **1993**, *98*, 5648−5652. (b) Lee, C. T.; Yang, W. T.; Parr, R. G. *Phys. Rev. B: Condens. Matter Mater. Phys.* **1988**, *37*, 785−789. (c) Vosko, S. H.; Wilk, L.; Nusair, M. *Can. J. Phys.* **1980**, *58*, 1200−1211. (d) Stephens, P. J.; Devlin, F. J.; Chabalowski, C. F.; Frisch, M. J. *J. Phys. Chem.* **1994**, *98*, 11623−11627.
(47) Binkley, J. S.; Pople, J. A.; Hehre, W. J. *J. Am. Chem. Soc.* **1980**, *102*, 939−947.
(48) (a) Rassolov, V. A.; Pople, J. A.; Ratner, M. A.; Windus, T. L. *J. Chem. Phys.* **1998**, *109*, 1223−1229. (b) Rassolov, V. A.; Ratner, M. A.; Pople, J. A.; Redfern, P. C.; Curtiss, L. A. *J. Comput. Chem.* **2001**, *22*, 976−984. (c) Ditchfield, R.; Hehre, W. J.; Pople, J. A. *J. Chem. Phys.* **1971**, *54*, 724−728.
(49) (a) Hay, P. J.; Wadt, W. R. *J. Chem. Phys.* **1985**, *82*, 270−283. (b) Wadt, W. R.; Hay, P. J. *J. Chem. Phys.* **1985**, *82*, 284−298. (c) Hay, P. J.; Wadt, W. R. *J. Chem. Phys.* **1985**, *82*, 299−310.
(50) Portmann, S.; Luthi, H. P. *Chimia* **2000**, *54*, 766−770.
(51) Beurskens, P. T.; Beurskens, G.; deGelder, R.; Garcia-Granda, S.; Gould, R. O.; Smits, J. M. M. *The DIRDIF2008 Program System*; Crystallography Laboratory, University of Nijmegen: Nijmegen, The Netherlands, 2008.
(52) Sheldrick, G. M. *Acta Crystallogr., Sect. A: Found. Crystallogr.* **2008**, *64*, 112−122.

DOI: 10.1021/acs.inorgchem.5b01315
Inorg. Chem. 2015, 54, 7645−7652